Joint 48th IEEE Conference on Decision and Control and
28th Chinese Control Conference
Shanghai, P.R. China, December 16-18, 2009

A maximum-likelihood detection scheme for rapid imaging of string-like samples in atomic force microscopy

Peter I. Chang and Sean B. Andersson
Mechanical Engineering, 1 Boston University, Boston, MA 02215
{itchang,sanderss}@bu.edu

Abstract— **In this paper, we present a sample-detection scheme designed for non-raster scanning in atomic force microscopy. The scheme utilizes a maximum-likelihood estimator applied over a moving window and enables the tracking of a string-like sample. By tracking, the tip is kept in proximity to the sample, reducing the total imaging time by eliminating the measurement of unnecessary information. We combine the new estimator with previously reported results and apply the algorithm in simulation to actual data obtained through a raster-scan image of DNA.**

I. Introduction

Atomic force microscopy (AFM) [1] has led to remarkable discoveries in the field of nanotechnology, molecular biology, medicine, materials science and many others. AFM is well known for its high spatial resolution. Because of this, and its ability to operate in liquid environments, it is well suited for the study of biological samples. As a result, AFM has led to improvements in our understanding of a variety of biological systems at the molecular level, including the structure and function of proteins, DNA, lipid films, and molecular motors [2]–[5]. Despite these successes, the applicability of AFM to study the dynamics in systems with nanometer-scale features is severely limited by the AFM's temporal resolution. For example, current commercial AFMs generate a single image in the order of minutes. Due to the wealth of dynamic phenomena with time scales much faster than this, there is great interest in improving the temporal resolution of the instrument.

To achieve this improvement, researchers have followed two main approaches: alternative physical designs (e.g. [6]–[8]) and advanced control technology (e.g. [9]–[11]), as well as combinations of both [12]. These schemes, however, treat the AFM system as an "open-loop" imaging device and continue to utilize the raster scan pattern as the basic scanning routine.

Our work approaches the goal of improved temporal resolution in a different manner - through non-raster scanning. By using the information collected by the instrument to adjust in real-time the measurement process, a more rational sampling can be achieved. Combining the measured data with *a priori* knowledge about the sample allows us to design feedback control laws that keep the tip in the vicinity of the sample, thereby reducing the imaging time by reducing the amount of measurements needed. Here we focus on string-like samples such as DNA, microtubules, and other biopolymers.

The core algorithm, briefly described in Sec. II, has been previously described in [13], [14]. Here we develop a maximum-likelihood scheme for detecting the underlying sample in the data captured through our tracking approach. Because our primary interest is in the imaging of biological samples, our discussion centers on the intermittent contact (or tapping) imaging mode, although the scheme is easily applied to other imaging modalities as well. We then illustrate the overall scheme by combing the elements of the algorithm, including the use of theoretical bounds for control parameter selection to guarantee tracking [15], to a data set from a traditional AFM raster-scan of a DNA strand.

II. Non-raster scan method with smooth scan trajectory

The raster-scan pattern can be viewed as an open-loop scheme for the trajectory of the AFM tip in the plane. As illustrated in Fig. 1, our non-raster scan method closes the high-level control loop of the AFM system to steer the tip in close proximity to the underlying string-like sample.

We model the string-like sample as a planar curve whose evolution in the plane is governed by the curvature. Given an estimate of the curvature and the tangent to the curve at the current point, the future evolution of the curve, at least locally, can be predicted by solving the Frenet-Serret frame equations to yield a predicted curve $r(s)$ where s is the arclength along the sample.

978-1-4244-3872-3/09/$25.00 ©2009 IEEE

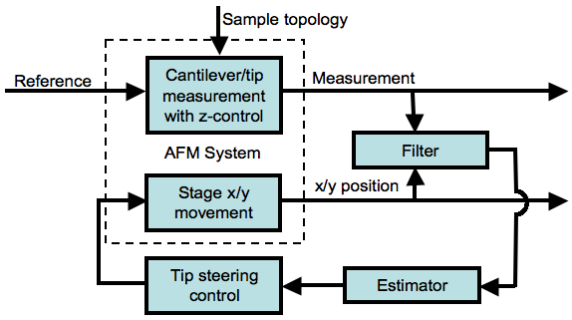

Fig. 1. Closing the high-level control loop. The measurements acquired by the tip are filtered and then used to estimate the parameters of the tip steering control. In the current paper, this controller drives the tip in a sinusoidal pattern along the string-like sample.

We define a scan pattern along this predicted curve by setting the tip trajectory x_{tip} to

$$x_{tip}(s(t)) = r(s(t)) + A\sin(\omega s(t))q_2(s(t)) \qquad (1)$$

where q_2 is the normal vector to the curve r, A is the scan amplitude, and ω the spatial frequency. As the tip moves, the measurements are used to continually estimate the path of r, leading to a scan pattern as shown in Fig. 2. Details can be found [14].

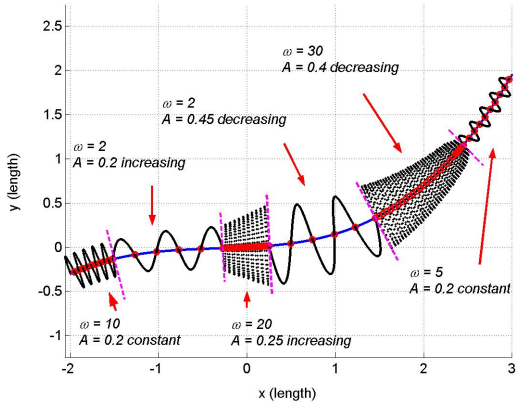

Fig. 2. Smooth non-raster scan pattern. The underlying curve (blue) is not known in advance but is estimated based on measurements obtained along the tip trajectory (black). Image from [14].

III. Detection Scheme

The tip trajectory x_{tip} is designed so that it periodically crosses the underlying sample. This allows us both to image the sample as well as to track it. In order to implement the tracking, an estimate of the location of the sample point r_{k+1} in the scan is needed. (Here the index k indicates the sample number along the path.) There are various techniques available to provide estimates of the sample location. For example, in [16] a high-speed detection scheme is introduced that relies on the transient dynamics in the cantilever when the tip transitions onto the sample. In this work, we are interested in using the measured data for generating images and therefore assume the measured signals (height, amplitude, phase) are available and of sufficient quality for detection.

In general, for string-like samples the tip will move up onto the sample, cross over, and then step down, as illustrated in Fig. 3. (We note that it is straightforward to extend the scheme presented below to boundaries, such as along a cell or along a crystal, in which the tip would only move up onto the sample during the portion of the scan illustrated in the figure.) The responses of the measured signals to this crossing are different for the height, amplitude and phase signals. For example, height increases as the tip steps onto the substrate and decreases as the tip steps down while the amplitude signal undergoes a brief decrease in its magnitude on the step up until the control loop responds to the disturbance, and a brief increase for the step down. These changes create a unique shape for the trace of the signals, and we use these shapes to identify the location of our underlying sample.

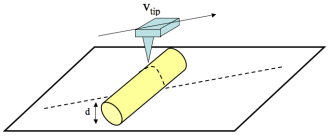

Fig. 3. Illustration of AFM tip crossing a string-like sample. The tip is moving at a speed v_{tip}, crossing the string-like sample at an arbitrary angle relative to the direction defined by the tangent vector of the string. The sample has an height of d.

In this paper, we design the detection scheme based on the height data measured, but it can easily be extended to the other signals. Since height data are measured sequentially along the scan trajectory, the sequence for N measurements along a segment of the scan can be modeled as:

$$z_j = h_j + v_j, \quad j = 1, 2, \cdots, N \qquad (2)$$

where z_j denotes the measured height, h_j the actual value, v_j the measurement noise, and the subscript j indexes the discrete sampling of the AFM along the scan trajectory. We assume the noise process is white with a zero mean, variance σ_v^2 Gaussian distribution. Other noise models can be used.

Equation (2) can be rewritten in vector form to yield

$$Z = H + V, \quad V \sim \mathcal{N}(0, \sigma_v^2 \mathbb{I}), \tag{3}$$

where Z is the measured height data, H the actual height, and V the modeled Gaussian white noise process.

A. Maximum likelihood estimator

We have chosen the maximum likelihood (ML) approach to detect the crossing points within the measured data. Depending on the sample that the AFM tip is crossing and the velocity at which the tip is traveling, one can model the crossing pattern with different shapes. In this paper we focus on a square function derived from subtracting one Heaviside function from another, the Heaviside function is defined as:

$$\mathbb{1}(s - s_0) = \begin{cases} 1, & s \geq s_0, \\ 0, & \text{otherwise.} \end{cases}$$

In our setting, s is the running arclength parameter used in our non-raster scan method, and s_0 denotes the position where the step up occurs.

We model the crossing pattern using a square function given by

$$h(s; \phi^*) = h^*(\mathbb{1}(s - s_0^*) - \mathbb{1}(s - (s_0^* + \rho^*))), \tag{4}$$

where $\phi^* = \{s_0^*, h^*, \rho^*\}$ is the collection of parameters controlling the shape of this function, with the superscript $(^*)$ denoting the true (unknown) value. In this vector, s_0^* represents the left edge of the square, h^* is the height of the sample, and ρ^* denotes the width of the square function. We note that this shape model can be adjusted to include a slope that accounts for the image tilt common to AFM.

The string tracking algorithm uses a single point to represent the position of the string-like sample in the scan. One can choose this point to be anywhere along the width of the sample, including either of the two edges. This point, however, should be the same along the string; that is, if one chooses the left edge for one crossing then the left edge should be used for the entire string.

To use the shape function with the sampled height data, we represent the square function (4) in discrete form as

$$h_{\phi^*}(j) = \begin{cases} h^*, & j^* \leq j \leq j^* + \rho_n^*, \\ 0, & \text{else,} \end{cases} \tag{5}$$

where j^* denotes the position where the step up begins, and the lower script for ρ_n^* denotes the width using the subindex n for discrete values.

The ML estimator is given as

$$\hat{\phi} = \arg\max_{\phi} p(Z|\phi) \tag{6}$$

where $p(Z|\phi)$ is the conditional probability distribution function (PDF) for obtaining the measurement Z given $\phi = \{h, j, \rho_n\}$.

In general, one solves (6) to determine the best estimate of the parameter ϕ. To simplify the optimization problem we can take advantage of *a priori* information about our sample. For example, the measured height of DNA in air is about 1.5 nm while in liquid it is 1.8 nm [17]. Using this knowledge and through scaling, we set the value of h^* to one.

From (3), the PDF in (6) is given by

$$p(Z|\phi) = \alpha \exp\left(-\sum_{j=1}^{N} \frac{(Z(j) - h_\phi(j))^2}{2\sigma_v^2} \right), \tag{7}$$

where α is the scaling factor of the Gaussian. Expressing this in terms of the log likelihood yields

$$\hat{\phi} = \arg\min_{\phi} \sum_{j=1}^{N} (Z(j) - h_\phi(j))^2. \tag{8}$$

In most cases, the measurement sequence collected along the scan trajectory consists of only a small number of points. Thus, this optimization problem can be solved rapidly through a simple numerical search.

Generally, for the tracking algorithm we are concerned primarily with the position of the string and not in the width ρ_n. We can then use a simpler shape model in which the width of the square function is set to zero, yielding

$$h_\phi(j) = \begin{cases} 1, & j = j^*, \\ 0, & \text{else.} \end{cases} \tag{9}$$

The ML likelihood estimation then reduces to the search for just one parameter, namely j^*. This shape function is particularly useful when the number of measurements in the trajectory are small. This is the case for string-like samples when the tip speed is large.

B. Moving window framework

In the non-raster scan pattern in (1), the tip is constantly moving in a sinusoidal pattern across the sample. In order to use the ML detection scheme, it is necessary to select proper segments of the continuous evolving curve for the N discrete data sets for detection. We have chosen a moving window framework illustrated in Fig. 4, to provide for a continuous update on the evolving tip trajectory and to estimate in real

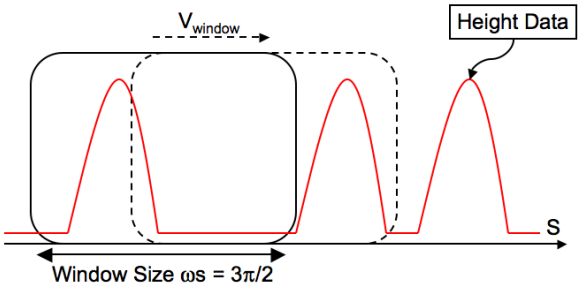

Fig. 4. Illustration of the moving window framework for ML estimation. The window size is chosen to guarantee that there is at least one string crossing inside at all times.

time the position of the sample in the scan as height measurements are acquired.

The size of this data "window" should be selected with care to ensure proper detection and avoid loss of tracking. The window frame should be large enough to ensure that there is indeed a crossing of the sample in the data set. Otherwise the data will consist of only noise and substrate, leading to false detection and erroneous parameter estimation in the tracking scheme. It is also important, however, to avoid a window size that is too large since the computational time for solving (8) is related to the amount of data. As a result, we choose the window size to be three-quarters of the spatial sinusoidal period, that is $\omega s \in [\omega s_o - 3\pi/2, \omega s_o]$ where s_o is the current position of the tip with respect to arclength.

The ML detection scheme thus proceeds as follows. To initialize, we first move the tip along the first three-quarters of a period of the tip trajectory to acquire a complete data set in the window frame. We then use the ML estimator to estimate the crossing position. We record this crossing location and return its actual position to the tracking algorithm. Based on this information, the tracking algorithm updates the estimate of the string sample and therefore the scan pattern. As the tip continues to move, we update the window frame and repeat the process. Note that the new window contains only a few new points and in general the detected crossing is the same as before. We therefore compare the new detected point with the previous one. If the difference is large enough, we update the position and send it to the tracking algorithm. Otherwise, we ignore the detected crossing.

IV. Example

We show here an example of applying the string-tracking scheme to data from an AFM image of DNA. The image was taken from the web site of Asylum Research [18]. As shown in Fig. 5, we selected a portion of the image that is approximately 500 nm by 500 nm, with 400 pixels in each direction. This corresponds to a resolution of 1.25 nm for each pixel. On the figure we also indicate the region to which we will apply the tracking algorithm. This portion was chosen as it contains a long strand with significant curvature and because it does not lie close to another strand of DNA (as in the left portion of the figure). We note that if there are two portions close together, then the tracking algorithm will still track the DNA but currently we cannot guarantee which strand will be followed after they separate. This question is the subject of ongoing research.

We incorporated the detection scheme presented in this paper with the tracking algorithm in [14]. The choice of scan parameters (A, ω) was guided by results in [15] (see IV-A). Note that the algorithm does not know *a priori* any information about the location of the DNA strand other than an initial condition. In practice, such an initial condition can be determined using an initial fast but rough scan or through simply scanning until a sample is detected. See [14] for more details.

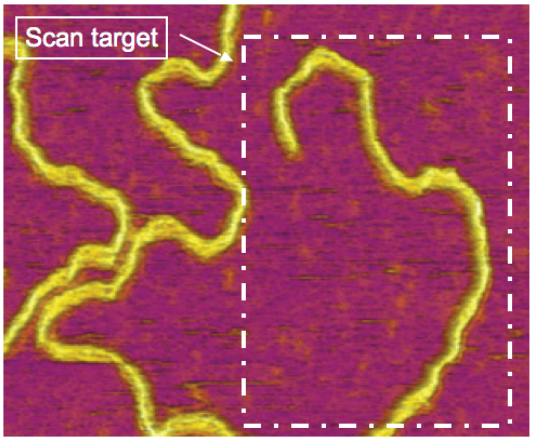

Fig. 5. DNA image data used for scan example. Image from [18].

A. Scan amplitude and scan frequency

Following our earlier work of [15], we can select the two main scan parameters, A and the spatial frequency ω, to guarantee that the algorithm will track the sample. This is done as follows.

First, we select the amplitude to ensure the sample is completely crossed during each spatial period of the sinusoid. In this case we need only select A larger than the known width of the sample. Here we choose $A =$

2.5 nm for a total scan width of 5 nm, significantly larger than the approximately 2 nm size of DNA.

We must then choose ω. This parameter serves as the resolution in the image and thus it should be chosen large enough to produce the desired resolution along the DNA. Choosing it too large, however, increases the total path length of the tip trajectory and thus the overall imaging time. Finally, we must also ensure tracking of the strand, even through regions of high curvature. In [15] we derive theoretical bounds on ω as a function of the amplitude, A, and the curvature, κ. Hence in addition to A, we need to determine the maximum curvature on the string-like sample.

In general this can be determined from the physical constraints of the sample to be imaged. Known models for DNA (for example, the worm-like chain model in [19]) can be used. Alternatively, if an initial, low-resolution scan is performed, the maximum curvature can be estimated from the data. We follow that approach here and calculate the curvature in two regions of the strand, shown in Fig. 6. The two regions have curvatures of 13.02 and 9.58, respectively. The resulting minimum values of $f = \frac{\omega}{2\pi}$ that guarantee tracking are also shown. With this we choose $\omega = 2\pi 10$.

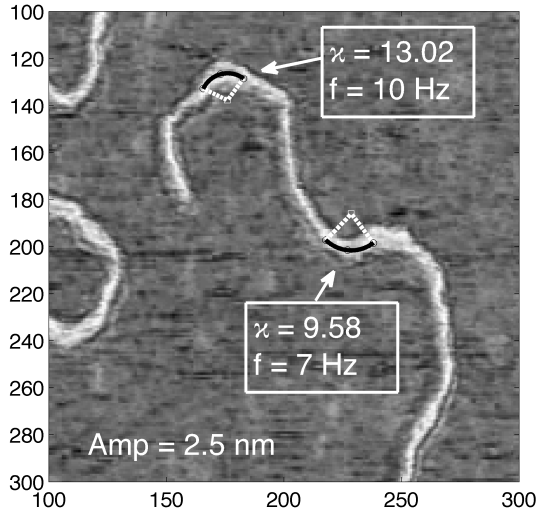

Fig. 6. Calculation on the minimum spatial frequency $\omega = 2\pi f$ that will guarantee tracking through curvature κ on the sample DNA image. Curvatures are calculated at two sharp turns to find the maximum value, and a suggested minimum frequency is calculated using the theoretical bounds with given the amplitude value. Note that the x and y axis are indices of the pixels.

B. Converting arclength to time

In order to avoid exciting unwanted dynamics in the scanning and measurement system, we choose to move the tip at a constant velocity of v_{tip} = 1 nm/unit time. Since the underlying curve, and thus the desired tip trajectory, is naturally described in terms of arc length, we need to determine the conversion between time and arclength as described in [14]. The relationship depends on the current curvature value and is illustrated in Fig. 7 for the selected scan parameters and for a curvature of zero. At every instant of time, the time value is then converted into the corresponding arclength value. This value is then used in the equation for the tip trajectory, (1) to determine the desired position of the tip.

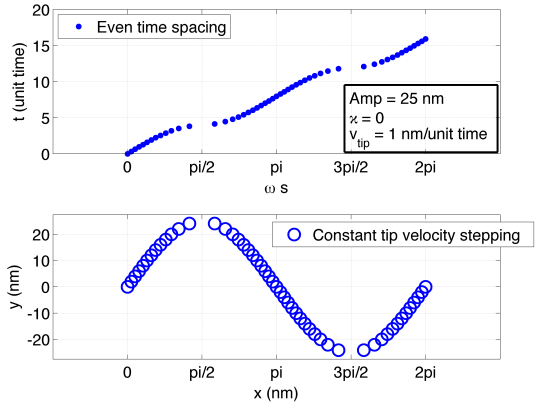

Fig. 7. Conversion between time and arclength at a constant v_{tip}. (Top) A regular sampling with respect to time yields an irregular sampling in arclength. (Bottom) The corresponding tip trajectory, illustrating the irregular spatial sampling.

Note that sampling at a fixed rate in time then corresponds to an uneven sampling in space as shown in the lower image in Fig. 7. The samples are denser near the portion of the trajectory corresponding to the location of the sample and sparser at the extremes of the trajectory. A constant sampling in space can easily be achieved by allowing for a varying tip speed.

C. Scanning

The result of scanning the strand according to our tracking algorithm is shown in Fig. 8. The non-raster scan is performed from the tip of the hook on the left of the DNA strand, and proceeds to the lower right part. The scan covers several consecutive turns in this DNA sample. The white dots indicates the trace of the tip trajectory x_{tip}, while the black squares indicates the crossing intersection points found by the moving window ML algorithm.

The height trace along the scan trajectory of this scan is shown in Fig. 9. It can be seen that the measured

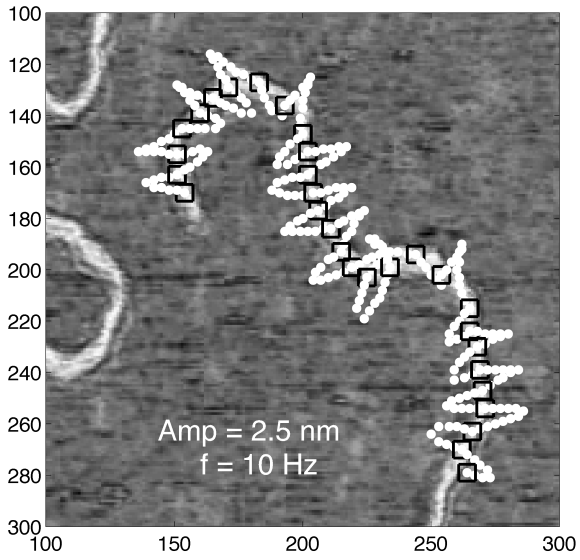

Fig. 8. Smooth scanning trajectory trace on the sample DNA image. The non-raster scan was initialized at the upper left part of the string, then scanned along the DNA strand towards the lower right corner, following its curvy path. The scan amplitude was 2.5 nm and the scan frequency was 10 Hz. These values are guaranteed to track this particular sample.

data itself is noisy. Our detection characteristic function essentially looks for a jump in the height signal, corresponding to when the tip crosses the underlying DNA sample. Note the value on y-axis is not in units of length due to image data conversion.

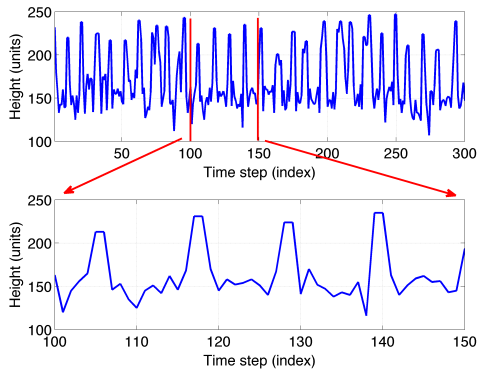

Fig. 9. Height data along the scan trajectory on the DNA image. The trace shows a noisy data set as we scan along the DNA strand. The crossing of the tip with sample occurs where the there is a jump in height measurement. The non-raster scan method identifies these regions with the moving window ML detection scheme.

ACKNOLWEDGEMENTS

This work was supported in part by a gift from the Agilent Foundation.

REFERENCES

[1] G. Binnig, C. F. Quate, and C. Gerber, "Atomic force microscope," *Phys. Rev. Lett.*, vol. 56, no. 9, pp. 930–933, 1986.
[2] D. J. Muller, "AFM: A nanotool in membrane biology," *Biochemistry*, vol. 47, no. 31, pp. 7986–7998, 2008.
[3] H. Janovjak, A. Kedrov, D. A. Cisneros, K. T. Sapra, J. Struckmeier, and D. J. Muller, "Imaging and detecting molecular interactions of single transmembrane proteins," *Neurobio. Aging*, vol. 27, no. 4, pp. 546–561, 2006.
[4] A. Alessandrini and P. Facci, "AFM: a versatile tool in biophysics," *Meas. Sci. Technol.*, vol. 16, pp. R65–R92(1), June 2005.
[5] N. C. Santos and M. A. R. B. Castanho, "An overview of the biophysical applications of atomic force microscopy," *Biophys. Chem.*, vol. 107, no. 2, pp. 133–149, 2004.
[6] S. C. Minne, J. D. Adams, G. Yaralioglu, S. R. Manalis, A. Atalar, and C. F. Quate, "Centimeter scale atomic force microscope imaging and lithography," *Appl. Phys. Lett.*, vol. 73, no. 12, pp. 1742–1744, 1998.
[7] T. Ando, T. Uchihashi, N. Kodera, D. Yamamoto, A. Miyagi, M. Taniguchi, and H. Yamashita, "High-speed AFM and nano-visualization of biomolecular processes," *Eur. J. Physiol.*, vol. 456, no. 1, pp. 211–225, 2008.
[8] K. K. Leang and A. J. Fleming, "High-speed serial-kinematic AFM scanner: Design and drive considerations," in *Proc. American Control Conference*, 2008, pp. 3188–3193.
[9] S. M. Salapaka and M. V. Salapaka, "Scanning probe microscopy," *IEEE Control Syst. Mag.*, vol. 28, no. 2, pp. 65–83, 2008.
[10] L. Y. Pao, J. A. Butterworth, and D. Y. Abramovitch, "Combined feedforward/feedback control of atomic force microscopes," in *Proc. American Control Conference*, 2007, pp. 3509–3515.
[11] S. Devasia, D. Chen, and B. Paden, "Nonlinear inversion-based output tracking," *IEEE Trans. Autom. Control*, vol. 41, no. 7, pp. 930–942, 1996.
[12] G. Schitter, K. Astrom, B. DeMartini, P. Thurner, K. Turner, and P. Hansma, "Design and modeling of a high-speed AFM-scanner," *IEEE Trans. Control Sys. Technol.*, vol. 15, no. 5, pp. 906–915, September 2007.
[13] S. B. Andersson, "Curve tracking for rapid imaging in AFM." *IEEE Trans. Nanobiosci.*, vol. 6, no. 4, pp. 354–361, 2007 Dec.
[14] P. I. Chang and S. B. Andersson, "Smooth trajectories for imaging string-like samples in AFM: A preliminary study," in *Proc. American Control Conference*, 2008, pp. 3207–3212.
[15] ——, "Theoretical bounds on a non-raster scan method for tracking string-like samples," in *Proc. American Control Conference*, 2009, pp. 2266–2271.
[16] S. M. Salapaka, T. De, and A. Sebastian, "Sample-profile estimate for fast atomic force microscopy," *Appl. Phys. Lett.*, vol. 87, no. 5, p. 053112, August 2005.
[17] F. Moreno-Herrero, J. Colchero, and A. M. BarÛ, "Dna height in scanning force microscopy," *Ultramicroscopy*, vol. 96, no. 2, pp. 167–174, 2003.
[18] [Online]. Available: http://www.asylumresearch.com
[19] C. Bustamante, J. F. Marko, E. D. Siggia, and S. Smith, "Entropic elasticity of λ-phage DNA," *Science*, vol. 265, no. 5178, pp. 1599–1600, September 1994.